Competing tunneling and capacitive paths in Co-ZrO_2 granular thin films

B. J. Hattink, A. Labarta, M. García del Muro, and X. Batlle
Departament de Física Fonamental, Universitat de Barcelona, Avinguda Diagonal 647, 08028-Barcelona, Spain

F. Sánchez and M. Varela
Departament de Física Aplicada i Òptica, Universitat de Barcelona, Avinguda Diagonal 647, 08028-Barcelona, Spain
(Received 1 October 2002; published 15 January 2003)

The ac electrical response is studied in thin films composed of well-defined nanometric Co particles embedded in an insulating ZrO_2 matrix which tends to coat them, preventing the formation of aggregates. In the dielectric regime, ac transport originates from the competition between interparticle capacitive C_p and tunneling R_t channels, the latter being thermally assisted. This competition yields an absorption phenomenon at a characteristic frequency $1/(R_tC_p)$, which is observed in the range 10–10 000 Hz. In this way, the effective ac properties mimic the *universal* response of disordered dielectric materials. Temperature and frequency determine the complexity and nature of the ac electrical paths, which have been successfully modeled by an R_t-C_p network.

DOI: 10.1103/PhysRevB.67.033402 PACS number(s): 83.80.Fg, 72.25.−b, 73.23.Hk, 73.50.−h

Granular films composed of magnetic nanoparticles embedded in an insulating matrix are currently the object of very active research because of their magnetic and transport properties, which have promising technological applications.[1] In addition, the rapid development of several film preparation techniques provides granular systems with a well controlled nanostructure, in which the interparticle transport processes and magnetic behavior of nanoparticles can be studied. In particular, dc transport properties of granular thin films have been widely investigated in the last decades[2] and explained in the dielectric regime at low electrical fields in terms of thermally assisted tunneling.[3] Although studies of the frequency behavior of tunneling junctions have been undertaken,[4,5] the ac response of granular metals in the dielectric regime is not yet properly characterized in the limit where the admittances rising from interparticle tunneling processes and interparticle capacitances become of similar magnitude. Previous experimental and theoretical works devoted to the study of the ac transport and optical properties of granular media have been almost exclusively focussed on systems for which tunneling processes can be neglected.[6–10] In these cases, a random network of capacitive and resistive bonds, which represent the insulating and metal components, respectively, has successfully modeled the ac response of granular metals.[6,7] In particular, scaling laws for ac magnitudes, based on percolation theory, have been proposed and experimentally verified in the metallic and dielectric regimes for negligible interparticle tunneling.[7–9]

In this paper, we report ac electrical measurements in granular thin films with competing tunneling and capacitive channels in the dielectric regime. Most of the observed ac properties mimic the universal response of disordered dielectric materials, but at much lower frequencies. In particular, as a direct consequence of the competition between tunneling and capacitive conduction, an absorption phenomenon is observed in the range 10–10 000 Hz, which is very much lower as compared to that corresponding to the *classical* optical properties in granular media.[10] This ac behavior is explained in terms of an R-C network in which each bond contains a parallel combination of randomly distributed values of a resistor (R) and a capacitor (C), where R is the tunneling resistance and C the interparticle capacitance.

Below the percolation threshold, the ac electrical transport between isolated metallic particles embedded in an insulating matrix is mainly due to two processes: (i) quantum electron tunneling between grains with separations of the order or less than one nanometer and (ii) the ac conduction by virtue of the capacitance between charged surfaces of neighbor particles, which can be thought of as electrodes of a complex network of capacitors. At low electrical fields, the first mechanism is temperature dependent, since it requires the thermal generation of charge carriers overcoming the Coulomb charging energy of the particles.[3] Assuming that the volume fraction x of the metallic component, is uniform within a region of a few particle diameters d it is reasonable to expect that l/d is a constant, l being the mean interparticle distance. Consequently, at each temperature the percolation path chiefly extends over the smallest particles whose Coulomb energies can be thermally activated. This is due to l/d being constant and the height of the tunnel barrier that increases exponentially with the interparticle separation.[3]

Contrarily, the capacitance is temperature independent and is always present between neighboring particles with their faced surfaces oppositely charged, no matter what their separation is. In fact, the highest capacitance occurs between the largest particles in spite of their large separation, since the capacitance for particles with similar size increases linearly with d (their capacitance is proportional to d^2/l with d/l being approximately constant throughout the system). Furthermore, ac transport between the largest particles is only possible by capacitance, since their corresponding large separation yields very high tunnel barriers.

The samples used in this study were 400 nm thick films composed of nanometric Co particles embedded in an insulating matrix of ZrO_2 stabilized with 7 mol. % Y_2O_3. The films were deposited at room temperature onto glass substrates by laser ablation of rotating targets comprised of sec-

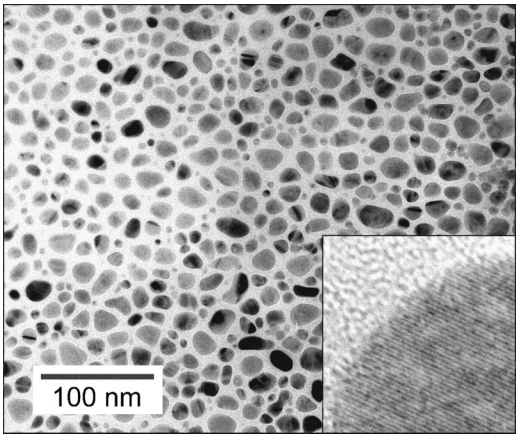

FIG. 1. Bright field TEM image for an annealed sample, displaying a distribution of Co particles in an Y_2O_3 stabilized ZrO_2 matrix. The inset shows parallel interference patterns inside the Co particles.

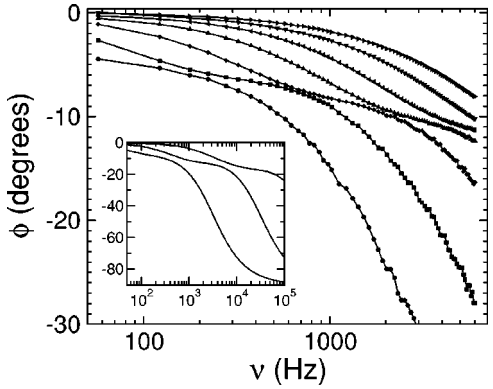

FIG. 2. The phase of the voltage drop across the sample versus frequency. From bottom to top, curves correspond to $T=29.0$, 40.5, 59.7, 90.3, 134.7, 214.7, and 290.1 K. The inset shows the corresponding results for a random R-C network. From left to right $x_r=0.95$, $R_t=2.5\times10^{14}\ \Omega$; $x_r=0.9$, $R_t=2.5\times10^{13}\ \Omega$; and $x_r=0.85$, $R_t=2.5\times10^{12}\ \Omega$. C_p and C_p' are fixed at $10^{-17}\ F$ and $50\ C_p$, respectively.

tors of zirconia and pure cobalt. Samples were reproducible as long as the preparation conditions were the same and the experimental parameters (e.g. energy fluence, size of the spot, and roughness of the target surface) were carefully controlled. Parts of the films were annealed at 575 °C for several hours. The average composition was determined by x-ray photoelectron spectroscopy and microprobe analysis. High resolution transmission electron microscopy (TEM) indicated the existence of crystalline Co particles (see the detail in Fig. 1) of round shape embedded in amorphous zirconia. The particle size distribution was determined by TEM as well as by fitting the low-field magnetic susceptibility (zero field cooling) and the high-temperature isothermal magnetization curves, to a distribution of Langevin functions. TEM showed sharp interfaces between the Co particles and insulating matrix with no detectable interdiffusion boundaries. Moreover, the amorphous matrix tends to coat the metallic particles, preventing the formation of aggregates even at relatively high Co concentrations. Thus, the medium is partially correlated, a fact which raises the effective percolation threshold. This allows us to obtain samples with a high metallic concentration consisting of nanometric isolated particles with small interparticle separations, avoiding the formation of filamentary clusters as observed in samples prepared by other methods near the percolation threshold.[8] The existence of metal-matrix interfaces of high quality is also confirmed by the observation of a quasitemperature independent magnetoresistance of about 7% in samples with Co-volume fractions close to $x=0.40$.[11] This value is in agreement with those found elsewhere for different Co-based granular systems[12] and corresponds to a spin polarization of 0.27, close to the expected value of $0.33-0.35$.[13] The ac electrical measurements were carried out by a four probe technique using a lock-in amplifier and an ac constant current source in the frequency range of 10 to 6500 Hz. Four parallel strips of copper separated by 0.7 mm were deposited on the sample's top surface as electrodes.

A deep insight in the ac electrical properties is gained by analyzing the phase ϕ of the voltage drop across the sample as a function of the frequency ν. The dependence of the $\phi(\nu)$ curves on the Co-volume fraction and annealing temperature will be published elsewhere.[11] In this paper, we focus on a sample with a Co-volume fraction $x=0.37$. Linear-logarithmic size distributions were obtained from low-field susceptibility, magnetization curves, and TEM images. For the as-deposited samples the mean diameter is $d=3.0\pm0.5$ nm with a width $\sigma=0.17$, whereas for the annealed samples $d=17\pm2$ nm and $\sigma=0.37$. Figure 2 shows $\phi(\nu)$, measured at different temperatures for the as-deposited sample. At high temperatures (around 290 K) and low frequencies, ϕ is roughly zero, corresponding to the current circulating essentially by interparticle tunneling through a resistive path. As ν is increased the admittance associated with the interparticle capacitance increases and the current progressively flows through capacitive paths which are in series and/or parallel configurations with respect to the tunneling channels, diminishing the phase of the voltage drop. At intermediate temperatures (see curves for 134.7, 90.3, 59.7, and 40.5 K in Fig. 2), a constant phase regime (CPR) is reached after a first phase drop similar to that observed at higher temperatures. The onset of this plateau occurs at frequencies at which the admittance associated with the capacitance between large particles becomes comparable to the tunneling conductance. In this way, capacitive short cuts are randomly inserted in the tunneling path, improving the electrical connectivity and thus favoring the current circulation through the resistive backbone. This regime is lost at higher frequencies, when the admittance due to the capacitance between small particles becomes comparable to the tunneling conductance and a significant part of the total current is flowing through this capacitive channel. The CPR shifts towards lower frequencies as the temperature is reduced because of the effective decrease of the tunneling conductance, as the amount of charge carriers is reduced. In particular, at 29 K, CPR has moved to frequencies below 10 Hz (see Fig. 2).

All the above features are also found in the ac response of a cubic random R-C network,[14] in which a fraction of the

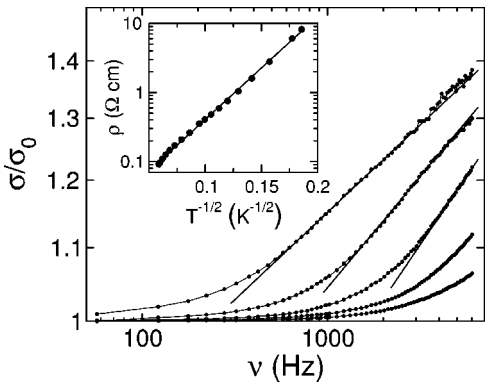

FIG. 3. Normalized conductance as a function of frequency. Temperatures are 59.7, 90.3, 134.7, 214.7, and 290.1 K from bottom to top. Straight lines indicate the CPR. The inset shows the zero frequency resistivity versus $T^{-1/2}$.

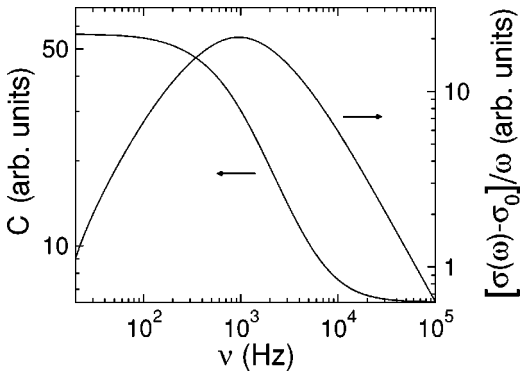

FIG. 4. Capacitance and loss peak as a function of frequency for a random R-C network with $x_r=0.9$, $R_t=2.5\times10^{13}\ \Omega$, $C_p=10^{-17}$ F, and $C_p'=50\ C_p$.

electrical bonds x_r are occupied by a parallel combination of a resistor R_t and a capacitor C_p (interparticle tunneling resistance and capacitance, respectively), and the rest by capacitors only, of higher capacitance C_p' (capacitance between the largest particles not electrically connected by tunneling). For 10 nm particles with a separation of 1 nm, R_t is estimated from experimental data on tunneling junctions to be in the range $10^{14}-10^{12}\ \Omega$ as the temperature varies from 30 to 290 K,[15] C_p is about 10^{-17} F (Ref. 16) and C_p' is assumed to be 50 C_p. The inset of the Fig. 2 shows $\phi(\nu)$ for a cubic lattice with 2900 electrical bonds, which was calculated with the WINSPICE program.[17] Three values of x_r and R_t have been used to simulate the effect of temperature, leading to a very good qualitative agreement with the experimental results. The thermal variation of the mean value of ϕ corresponding to the CPR can be understood from the logarithmic mixing rule[18]

$$\ln \sigma^* = \sum_n \ln \sigma_n^*, \tag{1}$$

where σ^* is the complex conductance of the system and σ_n^* is the conductance of the nth electric bond of the network. At intermediate frequencies at which the contribution of C_p can be neglected, a CPR of the conductance is obtained

$$\sigma^*(\omega) \approx (i\omega C_p')^{1-x_r}\ (1/R_t)^{x_r} \propto (i\omega)^{1-x_r}. \tag{2}$$

Therefore, ϕ in the CPR is simply $-(1-x_r)\ \pi/2$. From the experimental results (see Fig. 2) $(1-x_r)$ can be estimated to vary from about 0.05 at 29 K to about 0.13 at 290 K, indicating that as the temperature increases the fraction of effective resistive bonds is reduced. This is because higher thermal activation allows tunneling through smaller particles with higher charging energy, which reduces the total length of the resistive path.

The inset of Fig. 3 shows the thermal dependence of $\rho=\sigma_0^{-1}$, obtained from the experimental data by extrapolating the real part of the conductance $\sigma(\omega)$ to zero frequency. It is evident that except for a slight deviation at temperatures above 220 K, $\rho(T)$ varies as $\exp(2\sqrt{B/k_BT})$ with $B=25.3$ meV. Such a dependence is predicted[3] for thermally assisted tunneling and corroborates the existence of a tunneling path through the sample. In Fig. 3, the frequency dependence of $\sigma(\omega)/\sigma_0$ is depicted at different temperatures, which according to Eq. (2) follows a potential law with an exponent roughly within $0.05-0.13$ in the CPR frequency range.

It is worth noting that these electrical properties share with dielectric materials most of the features known as *universal* response.[19] In Fig. 4, it is shown that the total capaci-

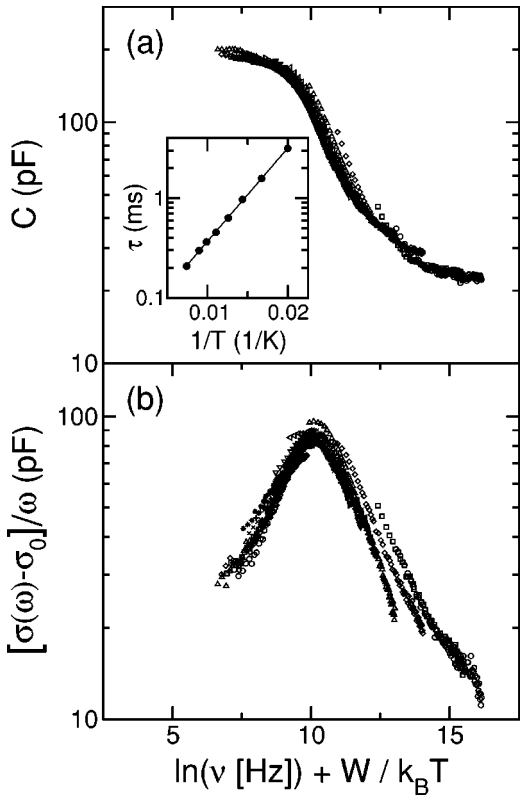

FIG. 5. Sample capacitance (a) and loss peak (b) as a function of $\ln(\nu)+W/k_BT$. The scaling factor W/k_BT is added to make the loss peak frequencies ν_p at different temperatures coincide. Different symbols correspond to T being varied from 29 to 275 K. In the inset $\tau=1/\nu_p$ is plotted versus $1/T$.

tance of the *R-C* network falls at intermediate frequencies following a power law and approaches the total interparticle capacitance of the system. At the same time, the dielectric loss defined as $[\sigma(\omega)-\sigma_0]/\omega$ develops a peak at the onset of the capacitance fall. For the experimental data, the peak position of the dielectric loss and the power law regime of the capacitance shift towards lower frequencies as the temperature is reduced. This is caused by the large thermal variation of the interparticle tunneling resistance originated from the change in the charge carrier amount. This thermal effect also changes the length of the resistive path, since at high temperatures the charging energy of the small particles may be overcome, creating new electrical paths with low tunneling barriers, and in this way, improving the system connectivity. In fact, the thermal dependence of the peak position of the dielectric loss is found to follow an Arrhenius law [see the inset of Fig. 5(a)], as expected for a thermal activation process, and takes place at a characteristic frequency of the order of $1/(R_t C_p')$. The activation energy deduced from this dependence is $W=18.6$ meV, a value which is comparable to that of the constant B in $\rho(T)$. By using $W/k_B T$ as a scaling parameter, all the curves corresponding to the capacitance and the dielectric loss at different temperatures collapse onto two master curves (see Fig. 5). These curves remarkably resemble those corresponding to the *universal* dielectric response,[19] but taking place in a lower frequency range than what is usually observed in dielectric materials. Moreover, both sides of the dielectric loss peak follow a power law, as expected for a universal response, with exponents close to 0.5.

No evidence of charge carrier trapping in the interfaces between metallic particles and the amorphous matrix has been observed. However, this effect only gives an additional contribution to the real part of the admittance, as previously observed in tunnel junctions,[5,20] but does not produce a loss peak. We cannot discard the occurrence of this phenomenon in our samples, but if present it would be hidden by the dominant contribution of the *R-C* competition.

In conclusion, we have showed that the ac absorption phenomenon in Co-ZrO_2 granular films originates from the competition between interparticle tunneling resistance and capacitance which takes place throughout a complex three-dimensional random *R-C* network. The inherent disorder of this network produces an effective *universal* response which is very similar to that observed in many disordered dielectric materials, but at much lower frequencies.

Financial support of the Spanish CICYT through the MAT2000-0858 and MAT99-0984 projects and the Generalitat of Catalonia through the 2000SGR00025 project are gratefully recognized.

[1] S. Ohnuma, H. Fujimori, S. Mitani, and T. Masumoto, J. Appl. Phys. **79**, 5130 (1996); M. Yu, Y. Liu, A. Moser, D. Weller, and D.J. Sellmeyer, Appl. Phys. Lett. **75**, 3992 (1999); W. Watanabe, T. Masumoto, D.H. Ping, and K. Hono, *ibid.* **76**, 3971 (2000).

[2] H. Fujimori, S. Mitani, and S. Ohnuma, J. Magn. Magn. Mater. **156**, 311 (1996); A. Milner, A. Gerber, B. Groisman, M. Karpovsky, and A. Gladkikh, Phys. Rev. Lett. **76**, 475 (1996); M. Holdenried and M. Micklitz, Eur. Phys. J. B **13**, 205 (2000).

[3] P. Sheng, B. Abeles, and Y. Arie, Phys. Rev. Lett. **31**, 44 (1973); B. Abeles, P. Sheng, M.D. Coutts, and Y. Arie, Adv. Phys. **24**, 407 (1975).

[4] P. Joyez, D. Esteve, and M.H. Devoret, Phys. Rev. Lett. **80**, 1956 (1998).

[5] K.T. McCarthy, S.B. Arnason, and A.F. Hebard, Appl. Phys. Lett. **74**, 302 (1999).

[6] X. Zhang and D. Stroud, Phys. Rev. B **52**, 2131 (1995); J.M. Laugier, J.P. Clerc, G. Giraud, and J.M. Luck, J. Phys. A **19**, 3153 (1986).

[7] D.J. Bergman and D. Stroud, Solid State Phys. **46**, 147 (1992).

[8] R.B. Laibowitz and Y. Gefen, Phys. Rev. Lett. **53**, 380 (1984).

[9] S. Bhattacharya, J.P. Stokes, M.W. Kim, and J.S. Huang, Phys. Rev. Lett. **55**, 1884 (1985); M.A. van Dijk, *ibid.* **55**, 1003 (1985).

[10] K.D. Cummings, J.C. Garland, and D.B. Tanner, Phys. Rev. B **30**, 4170 (1984).

[11] B. J. Hattink, X. Batlle, A. Labarta, F. Sanchez, and M. Varela (unpublished).

[12] M. Ohuma, K. Hono, E. Abe, H. Onodera, S. Mitani, and H. Fujimori, J. Appl. Phys. **82**, 5646 (1997); S. Sankar, A.E. Berkowitz, and D.J. Smith, Phys. Rev. B **62**, 14 273 (2000).

[13] M.B. Stearns, J. Magn. Magn. Mater. **5**, 167 (1977); R. Meservey and P.M. Tedrow, Phys. Rep. **238**, 174 (1994).

[14] J.C. Dyre, Phys. Rev. B **48**, 12 511 (1993); B. Vainas, D.P. Almond, J. Luo, and R. Stevens, Solid State Ionics **126**, 65 (1999).

[15] Y. Lu, R.A. Altman, A. Marley, S.A. Rishton, P.L. Trouilloud, G. Xiao, W.J. Gallagher, and S.S.P. Parkin, Appl. Phys. Lett. **70**, 2610 (1997); C.L. Platt, B. Dieny, and A.E. Berkowitz, *ibid.* **69**, 2291 (1997).

[16] S. Roy, Ph.D. thesis, University of Glasgow, 1994.

[17] WINSPICE by M. Smith, based on Spice 3F4 which was developed by the Department of Electrical Engineering and Computer Science at the University of Berkeley, http://www.willingham2.freeserve.co.uk/winspice.html.

[18] K. Lichtenecker, Z. Phys. **27**, 115 (1926).

[19] A.K. Jonscher, Nature (London) **267**, 673 (1977); A.K. Jonscher, J. Phys. D **32**, R57 (1999).

[20] J. Halbritter, J. Appl. Phys. **58**, 1320 (1985); A.F. Hebard, S.A. Ajuria, and R.H. Eick, Appl. Phys. Lett. **51**, 1349 (1987).